# ASSESSING SOIL EROSION SUSCEPTIBILITY FOR PAST AND FUTURE SCENARIOS IN SEMI-ARID MEDITERRANEAN AGRO-ECOSYSTEMS

Gianluigi Busico[1], Eleonora Grilli[1], Sílvia Carvalho[2], Mastrocicco Micol[1], and Simona Castaldi[1]

[1]Universita degli studi della Campania Luigi Vanvitelli Dipartimento di Scienze e Tecnologie Ambientali Biologiche e Farmaceutiche
[2]University of Lisbon CCIAM (CC Impacts Adaptation & Modelling)/cE3c Faculty of Sciences Lisbon Portugal

May 13, 2022

**Abstract**

The assessment of soil erosion rate, especially in agricultural lands, represents a fundamental tool for land management planning in the long-term period. In this study, the SWAT model was utilized to simulate soil erosion within a semi-arid watershed in South Portugal. The model was successfully calibrated and validated using real data of streamflow and river sediment transport in four hydrometric stations. Soil erosion susceptibility maps (historical and future) were realized to highlight the evolution of the phenomenon through time. The historical period was confirmed to be the worst one in terms of average soil erosion for each land use, followed by the Representative Concentration Pathways (RCPs) 8.5 and 4.5 scenarios. The main differences in soil loss among the two RCPs will be influenced by the slightly increasing trend of extreme events which will characterize the RCP 8.5, leading to a higher maximum value of soil erosion. Results highlighted the tendency to erosion of Leptosols and of the agro-forestry system ("montado"), which influenced the soil erosion susceptibility distribution of the whole basin. The study confirmed that Leptosols are the most subject to sediment loss due to their intrinsic characteristics, and that "montado" and farmed systems will negatively influence soil erosion rate if anti-erosion actions will not be adopted, stressing the need to identify all aspects responsible for land degradation in Mediterranean watersheds.

## ASSESSING SOIL EROSION SUSCEPTIBILITY FOR PAST AND FUTURE SCENARIOS IN SEMI-ARID MEDITERRANEAN AGRO-ECOSYSTEMS

Gianluigi Busico[1,*], Eleonora Grilli[1], Sílvia C. P. Carvalho[2], Micol, Mastrocicco[1], Simona Castaldi[1]

[1] University of Campania "Luigi Vanvitelli", Department of Environmental, Biological and Pharmaceutical Sciences and Technologies, Caserta, Italy.

[2] University of Lisbon, CCIAM (CC Impacts Adaptation & Modelling)/cE3c, Faculty of Sciences, Lisbon, Portugal.

[*]***Corresponding author: gianluigi.busico@unicampania.it***

GRAPHICAL ABSTRACT

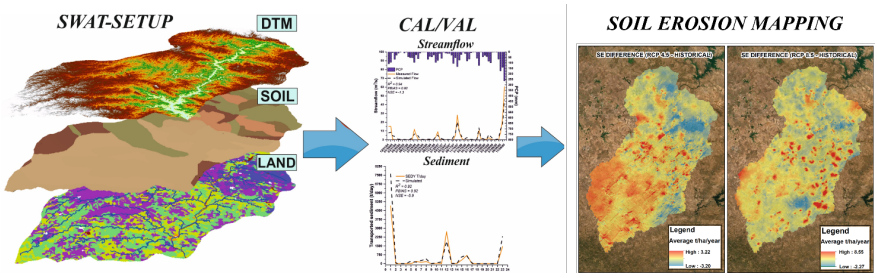



# ABSTRACT

The assessment of soil erosion rate, especially in agricultural lands, represents a fundamental tool for land management planning in the long-term period. In this study, the SWAT model was utilized to simulate soil erosion within a semi-arid watershed in South Portugal. The model was successfully calibrated and validated using real data of streamflow and river sediment transport in four hydrometric stations. Soil erosion susceptibility maps (historical and future) were realized to highlight the evolution of the phenomenon through time. The historical period was confirmed to be the worst one in terms of average soil erosion for each land use, followed by the Representative Concentration Pathways (RCPs) 8.5 and 4.5 scenarios. The main differences in soil loss among the two RCPs will be influenced by the slightly increasing trend of extreme events which will characterize the RCP 8.5, leading to a higher maximum value of soil erosion. Results highlighted the tendency to erosion of Leptosols and of the agro-forestry system ("montado"), which influenced the soil erosion susceptibility distribution of the whole basin. The study confirmed that Leptosols are the most subject to sediment loss due to their intrinsic characteristics, and that "montado" and farmed systems will negatively influence soil erosion rate if anti-erosion actions will not be adopted, stressing the need to identify all aspects responsible for land degradation in Mediterranean watersheds.


**Keywords: SWAT, soil erosion, South Portugal, Climate Change, hydrological model.**

# INTRODUCTION

Soil erosion (SE) is one of the major environmental issues in arid and semi-arid regions, especially in agricultural lands, identified as the areas with the highest average rate of soil losses around the world (Panagos et al., 2015a). SE represents the main cause of land degradation and desertification, with consequent loss of ecosystems services (Adhikari and Hartemink, 2016; Grilli et al., 2021; Zhao et al., 2013). The rate of SE is generally controlled by numerous factors and processes like wind, water inputs and balance, plant cover, geomorphology, soil type and anthropogenic activities (Arabameri et al., 2018; Bhattacharya et al., 2020). On a global scale, rainfall frequency and duration are the most important drivers of the observed and modeled SE rates (Borrelli et al., 2020; Burt et al., 2016). Especially in the last century, SE rates have strongly increased, leading to a world average soil loss rate of about 10.2 t/ha/year, which is expected to increase of 14% by the end of the twenty-first century (Yang et al., 2003), with climate change (CC) having a significant role in determining the severity of SE increase (IPCC, 2014). The Mediterranean region has been identified as one of the most vulnerable zones for SE, representing a CC 'hot-spot', due to the magnitude of the expected increase in temperature and anomalies in rainfall patterns (Giorgi, 2006; Giorgi and Lioniello, 2008; Zittis et al., 2019), such as higher frequency of extreme events, increased intensity of storms, extended drought periods, and higher risk of fire events (Moriondo et al., 2006; Busico et al., 2019). Additionally, the Mediterranean region is also characterized by centuries of anthropic disturbance, mainly related to agricultural and silvopastoral activities which might contribute to a substantial increase of SE rates (Raclot et al., 2016).

A robust quantitative SE assessment is a fundamental requirement for land management planning and policies aimed at stopping and reversing land degradation. Among the available tools, the empirical Universal Soil Loss Equation (USLE) (Wischmeier and Smith, 1978) and its revised version (RUSLE) (Renard et al., 1997) have been widely applied to determine the mean annual SE rates at regional and local scales (Mancino et al., 2016; Benavidez et al., 2018; Maltsev and Yermolaev, 2020). Panagos et al. (2015b) estimated the whole set of USLE parameters for Europe, significantly improving the potential applicability of this model. Despite their wide applicability, both methodologies still limit our ability to simulate soil deposition and to determine the location of sediment sources (Alewell et al., 2019). To overcome these drawbacks, a variety of river basin scale models were developed to simulate SE mechanisms and dynamics, such as the Water Erosion Prediction Model (WEPP) (Laflen et al., 1997), the Limburg Soil Erosion Model (LISEM) (De Roo et al., 1996), the European Soil Erosion Model (EUROSEM) (Morgan et al., 1998), and the Soil and Water Assessment Tool (SWAT) (Arnold et al., 1998; 2012) proposed by the United States Department of Agriculture (USDA). Among these, SWAT is one of the most appropriate models for assessing hydrological responses (water, sediment, and nutrient loss) to land use and CC in watersheds with different land covers, soil types, and management conditions (Bhatta et al., 2019; Busico et al., 2021, 2020; Golmohammadi et al., 2017; Tasdighi et al., 2018). In the last years, SWAT applicability was greatly increased thanks to the possibility of using a growing number of available global and regional datasets, making SWAT utilization much easier than before (Abbaspour et al., 2019). The proposed study is part of the European LIFE project "Desert-Adapt" (*http://www.desert-adapt.it/index.php/it/*) aimed at identifying appropriate land management strategies to reduced land degradation and desertification risk in semi-arid Mediterranean regions of Portugal, Spain, and Italy.

The goal of the present study is to evaluate if and how CC will affect SE rate within the Guadiana sub-basin, an arid area of Portugal (Alentejo) where four sites of the LIFE project are located (Fig. 1), assuming no change in land use (business as usual scenario, BAU) and considering two CC projection scenarios corresponding to different greenhouse gasses (GHGs) Representative Concentration Pathways (RCP 4.5 and RCP 8.5; IPCC, 2014). To meet this goal the operative steps of the study were: i) to create maps of SE susceptibility of the whole basin, ii) to assess its evolution over time (1980-2000, 2020-2040), and iii) to identify the areas more at risk and their current land uses to support adequate land management planning. Understanding the impact that CC will have on SE rates in the study area, and the identification of the most critical combinations of land management and environmental conditions which require special attention by farmers, is of paramount importance to define the most appropriate land management strategies to reduce current SE rates.

# MATERIALS AND METHODS

## Study area

The study area is located in the Alentejo region (Fig.1), southeastern Portugal. The Alentejo represents the largest region of Portugal, with a total area of about 31,500 km$^2$ hosting 5% of the entire Portugal population. Morphologically, the latter is an area with relatively low reliefs, where the elevation varies from 0 to 460 m above sea level (a.s.l.) (Fig. 2a). From a geological point of view, the basin mainly consists of metamorphic schists, greywackes, and conglomerates, distinguished by skeletal low productive soils (Chambel et al., 2007). The whole region has a typical Mediterranean – Continental climate, characterized by very hot and dry summers (Beck et al., 2018), with the highest amount of rain distributed during the winter season and drought periods (April-September) occurring during the year (Fig. S1). The mean annual precipitation ranges from 400 to 600 mm in the lowland and can reach up to 900 mm in mountain areas. In general, most of the annual rainfall is concentrated over 50-75 days (Ramos and Reis, 2001). The mean temperature is between 15.0 °C and 17.5 °C, while the potential evapotranspiration (PET) is generally higher than 1000 mm per year, causing a high water-soil deficit. Three main soil groups characterize the watershed: Leptosols are the most frequent, followed by Luvisols and Vertisols (Fig. 2c). The prevailing land cover (Fig. 2b) is

represented by annual rainfed crops (wheat and oats) followed by olive groves, cork oak (Quercus suber L.) woodlands alone or in combination with Quercus ilex L. and in some cases with Mediterranean shrubs. The "montado" ecosystems, representing the traditional agroforestry system of the Iberian peninsula with a savanna-like physiognomy, is characterized by grazing animals and by an open tree canopy woodland which can vary between 20 to 80 trees per hectare (mainly Quercus suber, Quercus ilex subsp. rotundifolia L) coexisting with grasses and scattered shrubs (Pinto-Correia and Mascarenhas, 1999). The entire region is presently under a high risk of desertification due to the presence of Leptosols (Fig. 2c), shallow and extremely gravelly soils naturally susceptible to erosion (IUSS Working Group WRB, 2015), to the intensive agriculture management and the overgrazing performed in recent decades (Roxo and Casimiro, 2004; Nùnes et al., 2008). The geomorphological, soil, and land cover characteristics of the four farms are presented in Table S1.

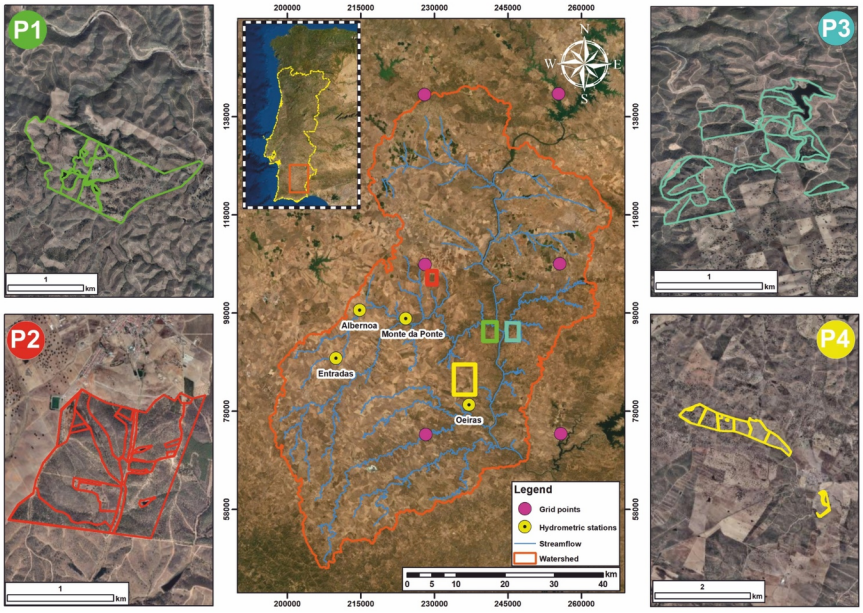


**Figure 1:** Geographical localization of the studied sites P1-P4, delimited by colored lines in the four side images and reported as rectangles in the central image, where the whole analyzed watershed is also shown.

## Data collection

For the realization of a complete SWAT model several datasets are required as inputs data. The Digital Elevation Model (DEM), needed for the delineation of the main watershed, river network, and sub-basin generation, was provided by the Shuttle Radar Topography Mission (SRTM), with a cell resolution of 10 x10 m. The land cover was obtained from the Corine Land Cover database (CLC, 2018), while the soil classification was extracted from Direcção-Geral de Agricultura e Desenvolvimento Rural (DGADR, 2013) with a scale of 1:25,000 (12.5 x 12.5 m). The information on soil characteristics, like saturated hydraulic conductivity (Ks), available water content (AWC), and bulk density (BD) were defined with the Harmonized World Soil database (FAO, 2012) a vectorial geodatabase obtained from a 30" resolution map and further refined using 3,000 soil columns from the World Soil Information Service (Batjes et al., 2017, 2020; Ribeiro et al., 2020) and literature data (Grilli et al., 2021), while other missing soil's parameters were obtained from SWAT's default dataset (Table S2). Data of streamflow and sediments load for the period 1985-1989 utilized to calibrate and validate the model were obtained from four hydrometric stations located inside the watershed named Albernoa, Monte da Ponte, Oeiras, and Entradas (Fig. 1) (SNIRH, 2006).

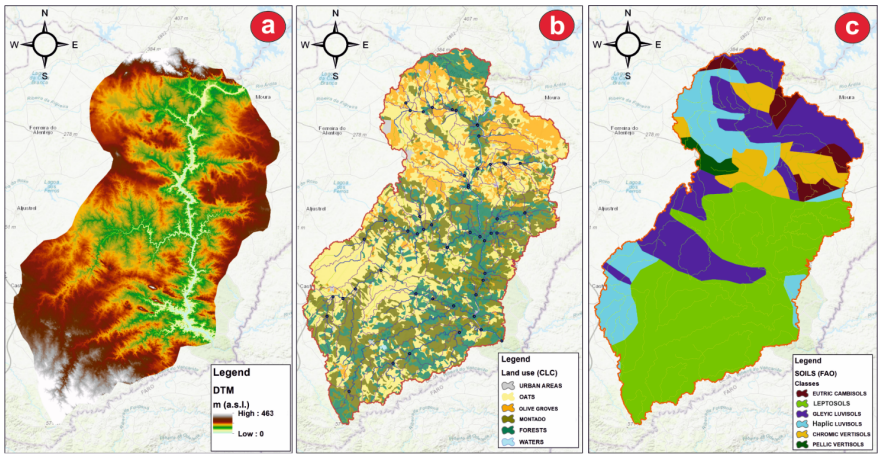


**Figure 2:** Physical characteristics of the analyzed watershed: a) morphology, b) land use classification (CLC, 2018), and c) soil types (DGADR, 2013).

***Climate dataset***

The time-series for calibration and validation purposes, including daily precipitation and max/min temperatures, were obtained from the dataset "Iberia01" (Herrera et al., 2012, 2016), which provides a dense network of stations over the Iberian Peninsula. All the data were extracted in seven grid points located inside or in the proximity of the analyzed basin. The high reliability of the spatial pattern of the reported variables is discussed by Herrera et al. (2019). These climate data were utilized for calibration and validation procedures as they overlap the simulation's period (1985-1989) of available data for streamflow and sediment transport.

As a reliable representation of precipitation's intensity and distribution is one of the predominant factors affecting the simulation results of hydrological processes, the choice of a representative climate dataset for the future scenarios is crucial to obtain accurate and reliable SE estimates. The datasets contemplated are based on currently available Regional Climate Models (RCMs), forced by different Global Climate Models (GCMs), which were used in the Fifth Assessment Report (AR5) of the Intergovernmental Panel on Climate Change (IPCC). The datasets were made available by the World Climate Research Program's CORDEX initiative (www.euro-cordex.net). In this study, the selected climate model, here called KNMI (i.e., RACMO22E driven by ICHEC-EC-EARTH), is in agreement with Soares et al. (2017), who assessed the performance of EURO-CORDEX historical (HIST) simulations to represent temporal and spatial patterns of precipitation over Portugal. Data were extracted from the RCM within 7 grid points, covering the period from 2020 to 2040.

## 2.3 Modelling Framework

SWAT model has the main purpose of simulating and predicting the effects of land management practices and CC on the hydrological cycle using different timescale input/output (daily, monthly, and yearly). The main step of the model consists in the creation of the hydrologic response units (HRUs), referring to all those portions of a territory characterized by unique land use, morphological, and soil attributes combination (Neitsch et al., 2000). All the model's outputs such as runoff, evapotranspiration, aquifer recharge, sediment, and nutrient loadings from each HRU are obtained using the input of climate, soil properties, topography, vegetation, and land management practices and further summarized to obtain the sub-basins loading. The outputs of runoff and sediment yield are calculated using a modified version of the curve number method (Brakensiek et al., 1984; USDA, 2004) or the Green–Ampt infiltration method, and the Modified Universal Soil Loss Equation (MUSLE) (Williams, 1995), respectively.

The SWAT model for the Guadiana river sub-basin was realized using ArcSWAT interface on ArcGIS 10.2 environment. The regime of SE for the whole watershed was evaluated with sequential steps.

First, all the physical characteristics of morphology, land cover, and soil properties were evaluated and used as main inputs for the setup of the SWAT model and to define the HRUs spatial distribution in the whole basin. The watershed automatic delineation tool divided the area of 37,233 $km^2$ in 99 sub-basins further discretized in 3000 HRUs. The HRUs were obtained intersecting five slope classes (<5, 5-10, 10-15, 15-20, >20), seven land cover categories (Fig. 2b), and six soil groups (Fig. 2c). The CLC classification was reclassified to match with the vegetation cover types present in the SWAT default database. Specifically, URMD was used to describe artificial settlements, OATS and OLIV for rainfed crops and olive plantations respectively, FRSE for rainfed forest, PINE for coniferous and mixed forest, while the "montado" system was represented using a combination of OAK and PAST (30% and 70%, respectively) using the SWAT code WPAS. Some parameters characterizing the typical Mediterranean vegetation were updated according to Nùnes et al. (2008). Concerning the soils' properties, all the information about Ks, AWC, texture, soil organic carbon (SOC), BD, and soil albedo utilized for the simulation are resumed in Table S1.

The meteorological data are the other necessary input for a proper SWAT evaluation. For this model, the meteorological data from "Iberia01" were used to run the model using daily data of precipitation and temperature to estimate runoff and actual evapotranspiration (AET) via the Hargreaves formula (Aschonitis et al., 2017). After the set-up procedure, the SWAT simulation, performed monthly, was divided into three blocks: i) a warm-up period of four years (1980-1984), ii) a calibration procedure from 01/1985 to 06/1987, and iii) a validation phase for the period 07/1987-12/1989 on four hydrometric stations for streamflow. For SE only two hydrometric stations were available (Monte da Ponte and Oeiras) with scattered daily data for the period 1984-1989. In particular, 38 daily data of SE were available, which were evenly split to perform calibration and validation analysis. Finally, the SWAT model was forced to simulate the HIST (1980-2000) and future period (2020-2040) using the chosen RCM (KNMI) under two different emission pathways (RCP 4.5 and 8.5).

The robustness of the methodology was investigated through an extensive calibration/validation procedure. A preliminary "trial and error calibration" was applied along with an "auto-calibration and validation". In the trial and error calibration, the fitted values of some parameters, such as groundwater "revap" coefficient (GW_REVAP), deep aquifer percolation fraction (RCHGDP), soil evaporation factor (ESCO), plant uptake compensation (EPCO), and deep aquifer percolation fraction (RCHGR_DP) were manually adjusted considering the results obtained from Nùnes et al. (2017) which performed a SWAT application in a nearby watershed. The other parameters responsible for streamflow and sediment load processes utilized for the auto-calibration were identified through an extensive literature review (Chen et al., 2019; Khelifa et al., 2017; Serpa et al., 2015), and are reported in Table 2. The standalone software SWAT-CUP via the Sequential Uncertainty Fitting version 2 (SUFI-2) algorithm (Abbaspour, 2015) was used for the auto calibration/validation. During the calibration phase, the SUFI-2 algorithm tries a different combination of the chosen parameters within their fixed range of variation (generally ± 25% of the initial value) and calculates the effect on the various fitting between the observed and simulated variables.

Three well known statistical indices were utilized to evaluate the simulation's results according to the performance values suggested by Moriasi et al. (2007) (Table S3): i) the coefficient of determination ($R^2$), ii) the Nash-Sutcliffe efficiency (NSE), and iii) the percent of bias (PBIAS); while the P-factor and R-factor values were investigated to account for model fit and uncertainties (Abbaspour et al., 2004).

A total of three thousand calibration runs, divided in six interactions of five hundred runs each, were performed until a satisfactory calibration was obtained. The values of SE in t/ha/year were obtained for the whole watershed. Furthermore, the values of SE for each HRU were spatialized and classified to obtain three SE susceptibility maps as to highlight the main changes over time and to identify those areas where SE will increase/decrease in the future. Finally, the results were analyzed to identify the mean yearly SE rate for each land cover category identified in the watershed.

# RESULTS

## SWAT model calibration and validation

The SWAT model successfully simulated both streamflow and sediment regime of the watershed (Fig. 3 and 4). For the streamflow, the calibration results showed a very good agreement between simulated and observed data, with high $R^2$, NSE, and good PBIAS in all available hydrometric stations (Fig. 4). Similarly, the statistical indices for the validation procedure were within the range of a "very good" model performance according to the model's performance criteria established by Moriasi et al. (2007) (Table S3). Considering the sediment load calibration, despite using randomly distributed sediment data, simulated and observed data showed a "very good" performance match for calibration and validation in both Monte Da Ponte (Fig. 4a) and Oeiras (Fig. 4b) stations. Regarding the streamflow simulation, the calibration/validation phases showed more than 70% of data bracketed by the 95PPU (P-factor [?] 0.70) with R-factors ranging from 0.15 to 0.3. For sediment, both Monte da Ponte and Oeiras reached a P-factor [?] 0.6 with an R-factor of 0.32 and 0.41, respectively. These results remarked a high model performance and efficiency for both variables.

A global sensitivity analysis was implemented to identify those parameters that strongly influenced the simulated flow and soil losses within those listed in Table 1. The significance of the sensitivity test was evaluated using the statistical index "p-value", automatically generated through the application of SUFI-2 algorithm. The results of the sensitivity analysis (Table 1, where the bold parameters represent the sensitive ones), indicated that the streamflow simulation was strongly dependent from DEEP_IMP, GW_DELAY, RCHGR_DP, and ALPHA_BF, while SLSUBBSN, USLE_K, and USCLE_C were the main parameters influencing the sediment loss simulation.

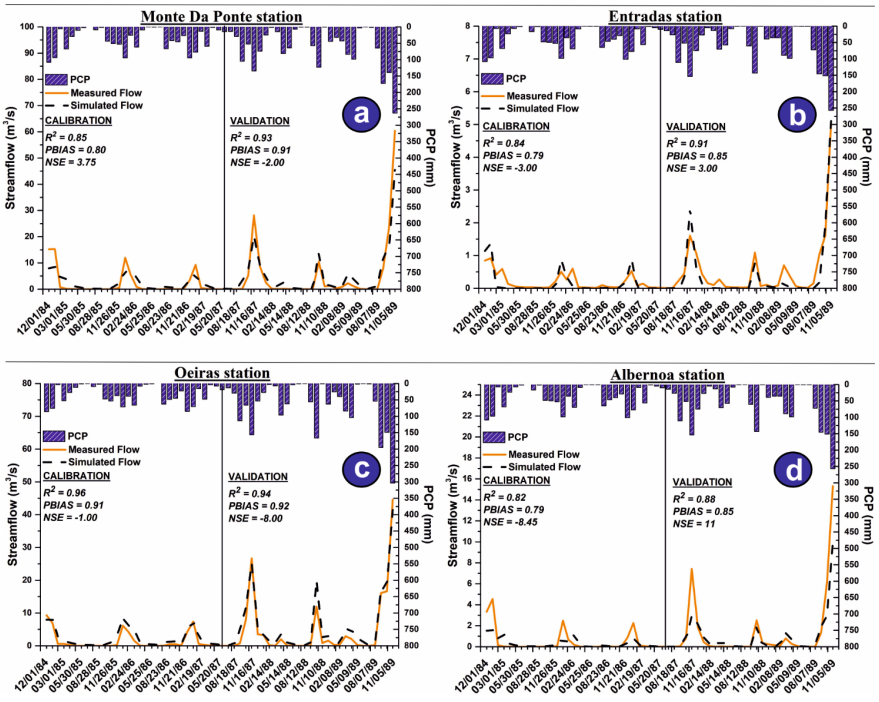


**Figure 3:** Calibration and validation for the streamflow simulation in the four hydrometric stations of the watershed.

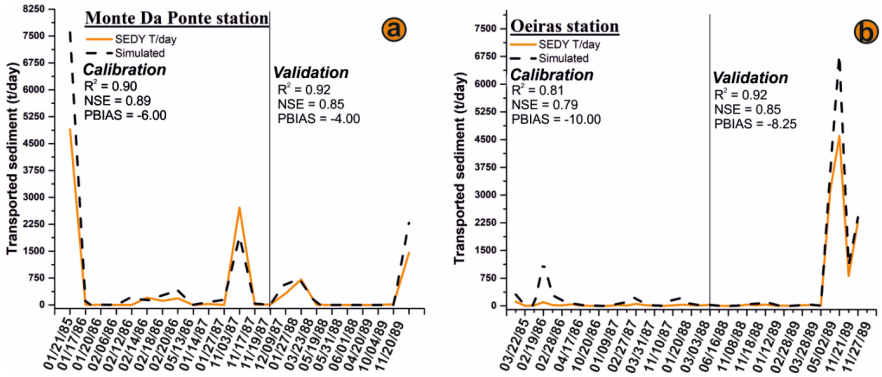


**Figure 4:** Calibration and validation for the sediment load simulation in the two hydrometric stations of the watershed.

**Table 1:** Parameter's description, sensitivity analysis results, and calibrated values for the SWAT simulation.

| Parameter | Cal. Value | Sensitivity | Description |
|---|---|---|---|
| SLSUBBSN | -0.083 | **0.01** | *Average slope length (m)* |
| USLE_K | 0.0082 | **0.00** | *USLE equation soil erodibility (K)* |
| USLE_P | 0.2 | **0.00** | *USLE equation support practice factor* |
| LAT_SED | 4837.5 | 0.45 | *Sediment concentration in lateral and groundwater flow (mg/L)* |
| CH_COV1 | 0.6875 | 0.32 | *Channel erodibility factor* |
| CH_BED_D50 | 5188.75 | 0.49 | *Particle size of channel bed sediment* |
| DEEP_IMP | 3000 | **0.00** | *Distance to the impervious layer* |
| GW_DELAY | 1 | **0.02** | *Groundwater delay time (days)* |
| ALPHA_BF | 0.13 | **0.00** | *Baseflow alpha factor (days)* |
| GW_REVAP | 0.2 | **0.03** | *Groundwater "revap" coefficient* |
| REVAP_MN | 1 | 0.20 | *Threshold depth of water in the shallow aquifer for "revap" or percolation to the* |
| RCHGR_DP | 0.5 | **0.05** | *Deep aquifer percolation fraction* |

## 3.2 Estimated soil erosion rates under climate scenarios

The simulated SE rates were averaged for the whole watershed over a period of 20 years providing a value of 3.3, 2.9, and 3.0 t/ha/year for the HIST, RCP 4.5, and RCP 8.5 scenarios, respectively. Maximum SE rates were also estimated providing a value of 25.3, 23.1 and 26.1 t/ha/year for the HIST, RCP 4.5, and RCP 8.5, respectively. The average value of SE for HIST, RCP 4.5 and RCP 8.5 in each HRU was used as a single point estimate to obtain a spatial distribution of the SE phenomenon over the entire basin, applying the kriging interpolation method. The spatialized data were grouped in 5 classes of SE susceptibility following the classification proposed by Panagos et al. (2015a): very low (SE [?] 1.0 t/ha/year), low (1.0 <SE[?] 2.5 t/ha/year), medium (2.5 <SE[?] 4.0 t/ha/year), high (4.0 <SE[?] 5.5 t/ha/year), and very high (SE > 5.5 t/ha/year). The susceptibility maps of the basin are showed in Figure 6. The SE susceptibility of the area during the reference period (HIST) shows the highest values in the central and southern parts of the study site, while the lowest values are estimated for the eastern border of the basin and in the northern area (Fig. 5a). In future conditions (RCP 4.5 in Fig. 5b and RCP 8.5 in Fig. 5c) the distribution of the SE susceptibility remains similar to the one of the HIST scenario, in terms of spatial distribution of the areas most prone to SE risk (Fig. 5a). In all cases, the portions of the basins most susceptible to SE are located in correspondence to Leptosols (Fig. 2c). The most interesting results were observed calculating the patterns of SE change between the future projections (RCP 4.5 and 8.5) and the HIST scenario (Fig. 6), obtained using a spatial difference through raster calculator in GIS environment.

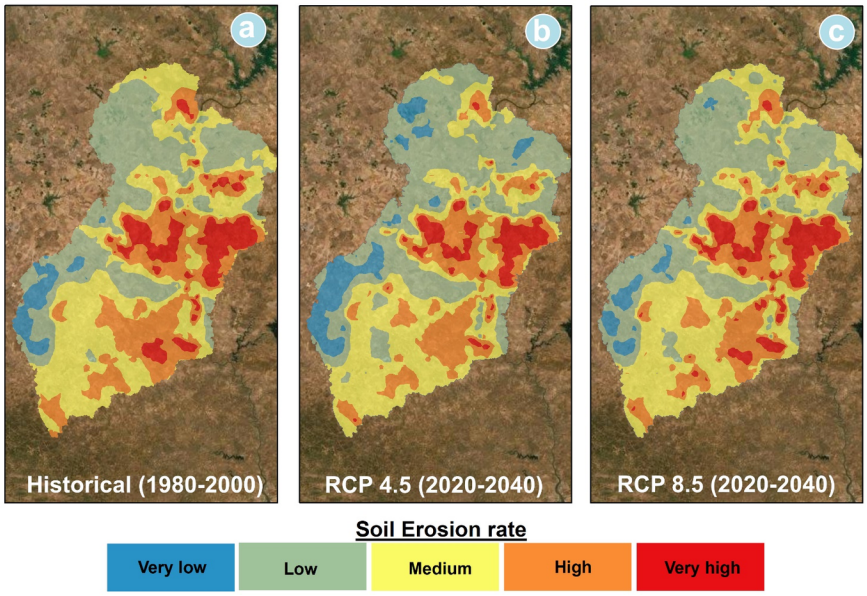


**Figure 5** : SE susceptibility maps for the Guadiana watershed: a) historical, b) future considering RCP 4.5, and c) future considering RCP 8.5.

The HIST-RCP 4.5 map shows a wider presence of areas characterized by an increase in absolute value of SE (t/ha/year) compared with HIST-RCP 8.5, especially in the south-west portion of the basin. On the other hand, HIST-RCP 8.5 map shows that under this extreme climatic scenario, there will be an increase of hotspots with high SE rates, probably because of the concentration of extreme rainfall events, while most of the basin will not experience big changes in SE susceptibility. Using the land cover variables as aggregation criterion, the SE values of the HRUs were averaged to homogenize soil and slope characteristics. According to the area characteristics, four main land covers were selected as the most representative of the basin, since together they occupy more than 95% of the entire territory: i) oats plantation (OATS), ii) evergreen forest (FRSE), iii) olive plantation (OLIV), and iv) the agroforestry system of "montado" (WPAS). Figure 7 shows the 20 years average (Fig. 7a) and 20 years maximum SE in t/ha/year (Fig. 7b) for each land cover. Results highlight that SE rate is in the order FRSE<OLIV<OATS<WPAS both for average and maximum values.

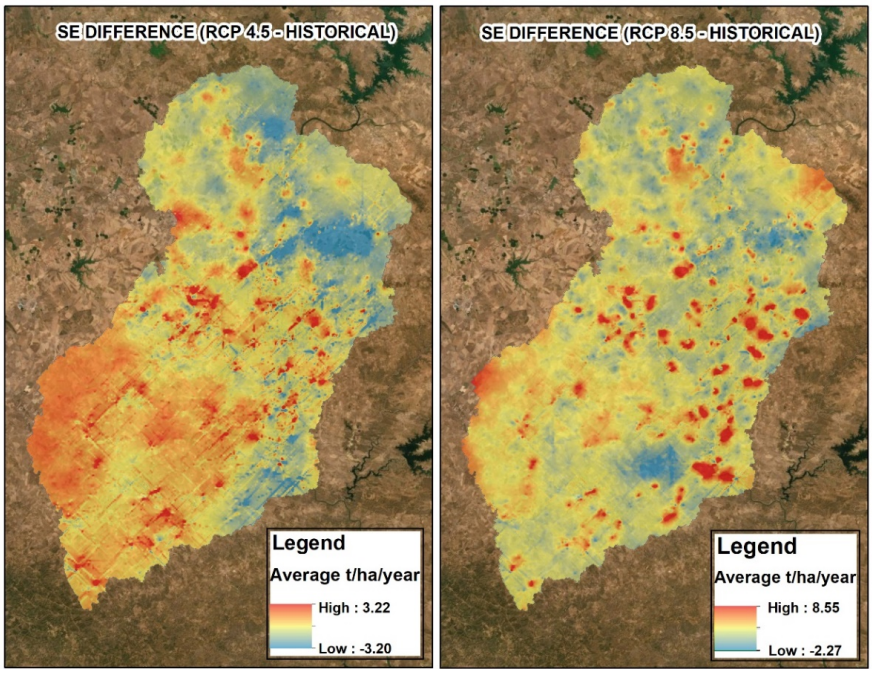


**Figure 6** : SE susceptibility maps net variation between future climate scenarios based on RCP 4.5 or RCP 8.5 and HIST with a BAU land management and cover in the studied Guadiana watershed.

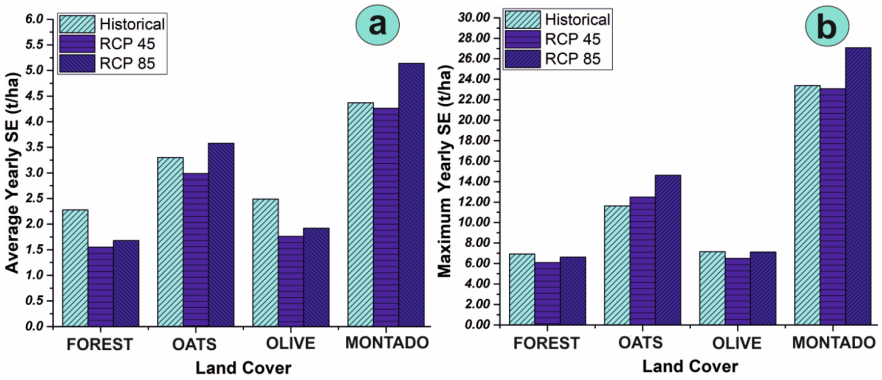


**Figure 7:** a) Average and b) maximum SE rate for each climate scenario.

**Table 2** : Average SE for each land use and SE susceptibility classification.

| | **Average SE (t/ha/year)** | **Average SE (t/ha/year)** | **Average SE (t/ha/year)** | | **t/** |
|---|---|---|---|---|---|
| **Land Cover** | Historical | RCP 4.5 | RCP 8.5 | All periods | <1 |
| **FOREST** | 2.44 | 1.84 | 1.86 | 2.05 | 1.0 |
| **OATS** | 3.45 | 3.12 | 3.60 | 3.40 | 2.5 |
| **OLIVE** | 2.54 | 1.98 | 2.06 | 2.09 | 4.0 |
| **MONTADO** | 4.42 | 4.12 | 5.19 | 4.53 | >5 |

Table 2 clearly shows that in the projected climatic scenario RCP 4.5 all land covers will slightly decrease

their SE rates. Conversely, the more extreme scenario RCP 8.5 would not change the SE rates in the areas with FRSE and OLIV but would slightly worsen the SE rates for the soils under OATS and WPAS, reaching SE rates even higher than the ones modelled for HIST.

# DISCUSSION

### 4.2 Projected soil erosion rates

Overall, the projected changes in SE rates with a BAU scenario under the future climatic conditions provided an average yearly SE rate for the next 20 years in the order of 2.9 and 3.0 t/ha/year for RCPs 4.5 and 8.5, respectively, both slightly lower than the HIST (1980-2000) average of 3.3 t/ha/year. The results agree with the projected climate indices for the area, which depict a future scenario of lowering precipitation and moderate extremes' increment. HIST and future values of SE were comparable with the SE classification proposed by Panagos et al. (2015a) for the Alentejo region, which reported SE rates from 2.0 to 5.0 t/ha/year; but they are slightly lower than the estimated average SE rate of 1.2 t/ha/year reported by Cerdan et al. (2010) for the whole area of Portugal. In term of soil stability and sustainability, Verheijen et al.(2009) indicated a tolerable range of SE between 0.4 and 1.4 t/ha/year, recommended to maintain a sustainable equilibrium between soil formation and soil loss for the European countries. Both HIST and future SE rates estimated in our sites are higher than this proposed tolerable range but they are in agreement with the results reported by Panagos et al. (2021) which forecasted an average SE for 2050 equal to 3.7 t/ha/year in agricultural areas across Europe. Moreover, the concomitant occurrence of dry and wet extremes due to CC might exacerbate the susceptibility to desertification of the entire region (Mirzabaev et al., 2019), increasing SE, decreasing crop yields and livestock productivity, with cascading impacts on food security and nutrition (EEA, 2019). Such SE rates represent a serious environmental issue in particular for the driest areas of Europe, like the Alentejo, under agricultural land use. Agricultural areas used for cropping or animal breeding are generally characterized by a significant removal of the C fixed via primary productivity and hence have less C available to feed SOC formation processes (Soussana et al., 2010; Whitehead, 2020), respect to natural environment. In drier conditions, primary productivity is further limited by water availability, further reducing the possibility for significant C input to the soil (ref). In these conditions SE rates greater than formation rates entail an irreversible loss of fertile topsoil, specifically organic carbon and nutrients, with a consequent decrease of soil-related ecosystem services (Steinhoff-Knopp et al., 2021), impacts on the global carbon cycle and increased GHGs emissions at watershed scale, especially in managed landscapes (Lal, 2019; Chappell et al., 2016).

In this respect, the SE results obtained in the simulation for the whole basin showed an improving SE trend, in particular under the most probable scenario RCP 4.5 (Table 2), with values that remained below 2 t/ha/year for FRSE and OLIV, which together cover 33% of the studied basin. However, the SE data reported in Table 2 are the average of land units characterized by the same land cover but having different parameters relevant for SE rate magnitude, like slope, soil type, SOC and other soil physical characteristics (Dissanayake et al., 2019). However, to improve land management it is more effective to represent the results in terms of SE susceptibility maps, rather than representing them as a simple average of the analysed SE for the whole basin. The SE susceptibility maps produced for the basin could help to provide the landowners of the four LIFE sites, not only with a clear picture of which areas would be more prone to SE, thus requiring higher attention, but also which areas might be more susceptible to further increment of SE risk in the future, thus needing more stable and long term management solutions. These maps showed a comparable pattern of the susceptibility classes for the HIST and the future scenarios (RCP 4.5 and 8.5) (Fig. 5) and clearly identified those areas which might be of major concern for land managers, but they were also used to evidence in which areas CC produced a substantial variation of SE with a BAU scenario (Fig. 6). The latter shows that under both future scenarios, the yearly SE average will be lower compared to the HIST scenario, with few exceptions mainly located in the central area of the basin. Considering the RCP 4.5 scenario, 95% of the most endangered areas are characterized by Leptosols, slope >10%, and a predominant land cover of

managed ecosystems ("montado" WPAS 50%, OAT 25%, OLIV 2%) and only a quarter covered by natural ecosystems (FRSE 23%), which makes these areas particularly in need to a dedicated land management plan to reduce SE effects. Moreover, comparing the maps of the SE difference between the HYST and the two future scenarios (Fig. 6), a very different average SE pattern is evident, which might be very relevant for management purposes.

According to this analysis, the magnitude of the SE rate in the studied basin changes significantly with factors such as soil erodibility, land cover, land management, and slope (Nùnes et al., 2011). Furthermore, in our study the SE susceptibility resulted more strongly influenced by soil and land use rather than morphology. In fact, the concomitant presence of WPAS on Leptosols determined the highest SE susceptibility of the whole central southern part of the basin. On one hand, Leptosols peculiarities (i.e., sandy texture, low soil's depth, and low SOC; Ebelhar et al., 2008), negatively impact soil erodibility determining low aggregates size and stability and slow plant growth. On the other hand, the presence of the montado system (WAPS) characterized by the exploitation of multiple resources (i.e., livestock, forestry, and crops) causes severe impacts on soil, increasing SE risk despite the presence of forestry and olive plantations (Shakesby et al., 2002). Indeed, continuous livestock trampling leads to soil compaction which reduces water infiltration with a consequent increase of surface runoff (Choelo et al., 2004), while intensive farming leads to loss of soil organic matter intensifying the degradation of such yet fragile soils (Nùnes et al., 2008). Continuous livestock grazing also reduces the vegetation cover that in turn negatively affects surface runoff under different rainfall intensity events, promoting soil loss. Schnabel et al. (2009) showed that for the grazed "dehesa" systems of Extremadura, an environmental system similar to "montando", a ground cover of at least 60% was necessary to protect the soil during exceptionally high intensity storms (I-30>40 $mm \cdot h^{-1}$). Whilst, a ground cover lower than 20% represented a threat, because soil loss occurred even in moderately intense storms. Mean SE rates related to sheet wash events was estimated to vary between 0.12 and 1.34 t/ha/year for 60% and 20% of ground cover, respectively. These estimates, corroborated by the studies of Kosmas et al. (1997) and Ceballos et al. (2002), clearly highlighted the key role of vegetation in land surface processes, which is why vegetation can be considered an*ecosystem services provider* (Guerra et al., 2016).

Finally, the low SE susceptibility across the north eastern border of the watershed match the OLIV (medium to low SE) and FRSE (low SE) distribution, on soil formations other than Leptosols. Accordingly, forests (FRSE) proved to exert a protective action on soil (Borrelli et al., 2017) exhibiting the lowest SE rates due to their capacity to intercept the rainfall by the tree canopies, independently of the soil type and morphology that characterize the area.

### 4.3 Soil erosion susceptibility management

The average SE rate calculated for the whole basin can be considered a relevant reference value for the planning of future management strategies for soil and water conservation (Yassoglou and Kosmas, 2000). For instance, Leptosols are well represented across Mediterranean coastal areas and considering that they are often intensively farmed, the results of this study can be easily transposed to these areas. The SE susceptibility maps can provide a significant and detailed indication for SE risk mitigation related to land use management. Such products can help in identifying those areas which would surely need the implementation of anti-erosion actions. Therefore, SE susceptibility maps can be an important tool for policy makers and farmers for watershed management. This assumption has been proved in several studies across India (Bhattacharya et al., 2020), Italy (Maruffi et al., 2022), Morocco (Markhi et al., 2018), and Ethiopia (Aga et al., 2018). According to the obtained results, several anti-erosion actions could be employed to overcome the increasing SE. Naturalization should be preferred to agricultural management and deforestation, especially on Leptosols, and this would be relevant even at relatively low slope (Englund et al., 2020). Permanent crops with greening management should be preferred to seasonal crops in areas under predominant agricultural management. With special reference to olive farming in Mediterranean regions, SE represents the principal environmental problem (Vanwalleghem et al., 2011), and both no-tillage soil management and cover crop development are proposed as adaptation strategies to CC impacts (Fraga et al., 2021). Overgrazing should be carefully avoided (Palm et al., 2014) introducing a holistic planned grazing (Savory and Butterfield, 1999) to promote

grassland self-regeneration. To make such an assessment effective on the long term, a projection of future SE risk is extremely useful for the protection and management of watersheds. The present study found that, despite both future scenarios will experience an impact in terms of increased average temperatures and a decline in precipitation respect to the historical scenario, the predicted increase of extreme events will lead to considerably higher SE maximum values for the RCP 8.5 scenario. Although this is a less probable scenario in view of the new EU policies to support climate actions and sustainable development, like the Green Deal and the Farm to Fork strategy, which complement the already existing PAC measures to support the agricultural sector, it interestingly shows the effect of intensification of extreme events on other ecosystem processes like SE, relevant for ecosystem sustainability, which requires a sensibilization action of land managers and landowners on this issues for a substantial reduction of soil loss from the most fragile areas of their land. Another relevant issue to consider is the significance of the estimated SE rates in terms of desertification and soil degradation risk, comparing the magnitude of SE rates with soil formation rates. Considering that the average 20 years values obtained from this study in all the time periods are higher than the desirable range of SE, comparable with the rate of soil formation (Verheijen et al., 2009), the implementation of management plans aimed at improving land use and promoting countermeasures to reduce SE become mandatory and urgent.

# CONCLUSIONS

In this study, the SWAT model was successfully applied to a Mediterranean watershed in south Portugal in areas under desertification risk to evaluate the effect of the current land management (BAU) on SE rates under present and future climatic scenarios. SE susceptibility maps allowed to appreciate the role played by a combination of relevant factors in determining SE rate, highlighting the suitability of SWAT model as a valid tool for simulating the impacts of climate variability on streamflow and sediment load and for creating extremely useful tool of land management for expert and not experts of the land management sector. Overall, our data show that future CC in the study area will create on average drier and warmer conditions with a slight increase in extreme events which will result in a very variable spatial distribution of areas under different SE risk, going from areas were SE will diminish compared to the actual climatic conditions and areas where the problem will further increase. The fact that the majority of these areas is currently under managed land cover, requires immediate attention ad adequate measures. This kind of tool might be of great help to inform and raise awareness in farmers, animal breeders and land owner. Results also underlined that, although the changing climate might exacerbate the conditions in the areas more at risk, in several areas of the basin SE rates with the actual conditions are already beyond the recommended threshold to maintain a sustainable equilibrium between soil formation and soil loss, posing serious risk of desertification in the near future.

**Supplementary materials** . Supplementary information related to the article is given in the following supplementary file (to be added by the journal).

**Author contributions** . The idea of the work was conceived by Gianluigi Busico, Micol Mastrocicco and Simona Castaldi, the data processing was made by Gianluigi Busico, Silvia C.P. Calvalho and Eleonora Grilli. The original draft was produced by Gianluigi Busico and while the quality data control was made by Eleonora Grilli and Silvia C.P. Calvalho. Final review, visualization and writing were completed by Micol Mastrocicco and Simona Castaldi.

**Competing interests** . The authors declare that they have no conflicts of interest.

**ACKNOWLEDGEMENTS**

The present study is supported by the EU project LIFE16 CCA/IT/000011. We thank the Associacao de Defesa do Patrimonio de Mertola for supporting during the field sampling. We also want to thank Dr. Joao Pedro Nunes for assisting in the preliminary model set up.

# REFERENCES


1. Abbaspour, K.C. (2015). SWAT-calibration and uncertainty programs. A user manual. Eawag: Swiss Federal Institute of Aquatic Science and Technology, Dubendorf, pp. 103.
2. Abbaspour, K.C., Johnson, A and Van Genuchten, M.T. (2004) Estimating uncertain flow and transport parameters using a sequential uncertainty fitting procedure. Vadose Zone J. 3(4), 1340–1352. Doi:10.2113/3.4.1340.
3. Abbaspour, K.C., Vaghefi, S. A., Yang, H., Srinivasan, R. (2019). Global soil, land-use, evapotranspiration, historical and future weather databases for SWAT Applications. Sci. Data 6, 263. Doi:10.1038/s41597-019-0282-4.
4. Adhikari, K., Hartemink, A.E. (2016). Linking soils to ecosystem services – a global review. Geoderma 262, 101-111. Doi:T10.1016/j.geoderma.2015.08.009.
5. Aga, A.O., Chane, B., Melesse, A.M. (2018). Soil erosion modelling and risk assessment in data scarce rift valley lake regions, Ethiopia. Water (Switzerland), 10(11) DOI:10.3390/w10111684.
6. Alewell, C., Borrelli, P., Meusburger, K., Panagos, P. (2019). Using the USLE: Chances, challenges, and limitations of soil erosion modelling. ISWCR 7(3), 203-225. Doi:10.1016/j.iswcr.2019.05.004.
7. Arabameri, A., Pradhan, B., Pourghasemi, H.R., Rezaei, K. (2018). Identification of erosion prone areas using different multi-criteria decision-making techniques and GIS. Geomatics, Nat. Hazards Risk 9(1), 1129-1155. Doi:10.1080/19475705.2018.1513084.
8. Arnold, J.G., Moriasi, D.N., Gassman, P.W., Abbaspour, K.C., White, M.J., Srinivasan, R., Santhi, C.R., Harmel, D., van Griensven, A., Van Liew, M.W., Kannan, N., Jha, M.K. (2012). SWAT: Model Use, Calibration, and Validation. Trans. ASABE 55(4), 1491–1508. Doi:10.13031/2013.42256.
9. Arnold, J.G., Srinivasan, R., Muttiah, R.S., Williams, J.R. (1998). Large-area hydrologic modeling and assessment: Part I. Model development. J. Am. Water Resour. Assoc. 34, 73–89. Doi:10.1111/j.1752-1688.1998.tb05961.x.
10. Aschonitis, V.G., Papamichail, D., Demertzi, K., Colombani, N., Mastrocicco, M., Ghirardini, A., Castaldelli, G., Fano, E.A. (2017). High-resolution global grids of revised Priestley–Taylor and Hargreaves–Samani coefficients for assessing ASCE standardized reference crop evapotranspiration and solar radiation. Earth Syst. Sci. Data 9, 615–638. Doi:10.5194/essd-9-615-2017.
11. Batjes, N.H., Ribeiro, E., van Oostrum, A. (2020). Standardised soil profile data to support global mapping and modelling (WoSIS snapshot 2019). Earth Syst. Sci. Data 12(1), 299-320. Doi:10.5194/essd-12-299-2020.
12. Batjes, N.H., Ribeiro, E., van Oostrum, A., Leenaars, J., Hengl, T., Mendes de Jesus, J. (2017) WoSIS: providing standardized soil profile data for the world. Earth Syst. Sci. Data 9, 1–14, Doi:10.5194/essd-9-1-2017, 2017.
13. Beck, H.E., Zimmermann, N.E., McVicar, T.R., Vergopolan, N., Berg, A., Wood, E.F. (2018). Present and future koppen-geiger climate classification maps at 1-km resolution. Sci. Data 5, 180214. Doi:10.1038/sdata.2018.214.
14. Benavidez, R., Jackson, B., Maxwell, D., Norton, K. (2018). A review of the (Revised) Universal Soil Loss Equation ((R)USLE): with a view to increasing its global applicability and improving soil loss estimates, Hydrol. Earth Syst. Sci. 22, 6059–6086. Doi:10.5194/hess-22-6059-2018.
15. Bhatta, B., Shrestha, S., Shrestha, P.K., Talchabhadel, R. (2019). Evaluation and application of a SWAT model to assess the CC impact on the hydrology of the Himalayan river basin. Catena 181, 104082. Doi:10.1016/j.catena.2019.104082.
16. Bhattacharya, R.K., Chatterjee, N.D., Das, K. (2020). Sub-basin prioritization for assessment of soil erosion susceptibility in Kangsabati, a plateau basin: A comparison between MCDM and SWAT models. Sci. Tot. Environ. 734, 139474. Doi:10.1016/j.scitotenv.2020.139474.
17. Borges, P.J., Fragoso, R., Garcia-Gonzalo, J., Borges, J.G., Marques, S., Lucas, M.R. (2010). Assessing impacts of common agricultural policy changes on regional land use patterns with a decision support system. an application in southern Portugal. For. Policy and Eco. 12(2), 111-120. Doi:10.1016/j.forpol.2009.09.002.

18. Borrelli P, Panagos P, Marker M, Modugno S, Schutt B (2017). Assessment of the impacts of clear-cutting on soil loss by water erosion in Italian forests: First comprehensive monitoring and modelling approach. Catena 149:770-781. https://doi.org/10.1016/j.catena.2016.02.017
19. Borrelli, P., Robinson, D.A., Panagos, P., Lugato, E., Yang, J. E., Alewell, C., Wupper, D., Montanarella, L., Ballabio, C. (2020). Land use and CC impacts on global soil erosion by water (2015-2070). PNAS USA 117(36), 21994-22001. Doi:10.1073/pnas.2001403117.
20. Brakensiek, D.L., Rawls, W.J., Stephenson, G.R. (1984). Modifying SCS hydrologic soil groups and curve numbers for rangeland soils. ASAE Paper No. PNR-84-203. American Society of Agricultural Engineers, St. Joseph, MI, USA.
21. Burt, T., Boardman, J., Foster, I., Howden, N. (2016). More rain, less soil: long-term changes in rainfall intensity with CC. Earth Surf. Process. Landf. 41, 563–566. Doi:10.1002/esp.3868.
22. Busico, G., Colombani, N., Fronzi, D., Pellegrini, M., Tazioli, A., Mastrocicco, M. (2020). Evaluating SWAT model performance, considering different soils data input, to quantify actual and future runoff susceptibility in a highly urbanized basin. J. Environ. Manag. 266, 110625. Doi:10.1016/j.jenvman.2020.110625.
23. Busico, G., Giuditta, E., Kazakis, N., Colombani, N. (2019). A hybrid GIS and AHP approach for modelling actual and future forest fire risk under CC accounting water resources attenuation role. Sustainability 11(24), 7166. Doi:10.3390/su11247166.
24. Busico, G., Ntona, M.M., Carvalho, S.C.P., Patrikaki, O., Voudouris, K., Kazakis, N. (2021). Simulating future groundwater recharge in coastal and inland catchments. Water Resour. Manag. 35, 3617–3632. Doi:10.1007/s11269-021-02907-2.
25. Ceballos, A., Cerda, A., Schnabel, S. (2002). Runoff production and erosion processes on a dehesa in western Spain. Geogr. Rev. 92(3), 333-353. Doi: 10.2307/4140914.
26. Cerdan, O., Govers, G., Le Bissonnais, Y., Van Oost, K., Poesen, J., Saby, N., Gobin, A., Vacca, A., Quinton, J., Auerswald, K., Klik, A., Kwaad, F.J.P.M., Raclot, D., Ionita, I., Rejman, J., Rousseva, S., Muxart, T., Roxo, M.J., Dostal, T. (2010). Rates and spatial variations of soil erosion in europe: A study based on erosion plot data. Geomorphology 122(1-2), 167-177. Doi:10.1016/j.geomorph.2010.06.011.
27. Chambel, A., Duque, J., Nascimento, J. (2007). Regional study of hard rock aquifers in Alentejo, south Portugal: methodology and results. In: Krasny J, Sharp JM (eds) IAH-SP Series. Taylor and Francis, 73–93.
28. Chappell, A., Baldock, J., Sanderman, J. (2016). The global significance of omitting soil erosion from soil organic carbon cycling schemes. Nat. Clim. Change 6, 187–191. DOI: 10.1038/nclimate2829.
29. Chen, Y., Xu, C.-Y., Chen, X., Xu, Y., Yin, Y., Gao, L., Liu, M. (2019). Uncertainty in simulation of land-use change impacts on catchment runoff with multi-timescales based on the comparison of the HSPF and SWAT models. J. Hydrol. 573, 486–500. Doi:10.1016/j.jhydrol.2019.03.091.
30. CLC: Corine Land Cover - Copernicus Land Monitoring Service (2018). Available online at: https://land.copernicus.eu/pan-european/corine-land-cover/clc2018 .
31. De Roo A.P.J., Wesseling C.G., Ritsema C.J. (1996). Lisem: A single-event physically based hydrological and soil erosion model for drainage basins. I: Theory, input and output. Hydrol. Process. 10(8), 1107-1117. Doi: 10.1002/(sici)1099-1085(199608)10:8<1107::aid-hyp415>3.0.co;2-4
32. DGADR: Direccao-Geral de Agricultura e Desenvolvimento Rural (2013). Solos, cartografiaeinformacao geografia.
33. Dissanayake, D., Morimoto, T., Ranagalage, M. (2019). Accessing the soil erosion rate based on RUSLE model for sustainable land use management: a case study of the Kotmale watershed, Sri Lanka. Model. Earth Syst. Environ. 5, 291–306. Doi:10.1007/s40808-018-0534-x
34. Ebelhar, S., Chesworth, W., Paris, Q., Spaargaren, O. (2008). Leptosols. In: Chesworth W. (eds) Encyclopedia of Soil Science. Encyclopedia of Earth Sciences Series. Springer, Dordrecht. Doi:10.1007/978-1-4020-3995-9_323.
35. EEA. (2019). European Environment Agency. Climate change adaptation in the agriculture sector in Europe. 108 pp. ISBN 978-92-9480-072-05 doi:10.2800/537176.

36. Englund, O., Borjesson, P., Berndes, G., Scarlat, N., Dallemand, J.F., Grizzetti, B., Dimitriou, I., Mola-Yudego, B., Fahl, F. (2020). Beneficial land use change: Strategic expansion of new biomass plantations can reduce environmental impacts from EU agriculture. Global Environ. Chang. 60, 101990. Doi:10.1016/j.gloenvcha.2019.101990.
37. FAO: Food and Agriculture Organization of the United Nations (2007). Available online at: http://www.fao.org/geonetwork/srv/en/metadata.show?id1/414116.
38. Fraga, H., Moriondo, M., Leolini, L., Santos, J.A. (2021). Mediterranean Olive Orchards under Climate Change: A Review of Future Impacts and Adaptation Strategies. Agronomy. 11, 56.*Doi:* 10.3390/agronomy11010056.
39. Golmohammadi, G., Rudra, R., Dickinson, T., Goel, P., Veliz, M. (2017). Predicting the temporal variation of flow contributing areas using SWAT. J. Hydrol. 54, 375–386. Doi:10.1016/j.jhydrol.2017.02.008.
40. Giorgi, F. (2006). CC hot-spots. Geophys. Res. Lett. 33, L08707. Doi: 10.1029/2006GL025734.
41. Giorgi, F., Lionello, P. (2008). CC projections for the Mediterranean region. Glob. Planet. Chang. 63, 90–104. Doi:10.1016/j.gloplacha.2007.09.005.
42. Grilli, E., Carvalho, S.C.P., Chiti, T., Coppola, E., D'Ascoli, R., La Mantia, T., Marzaioli, R., Mastrocicco, M., Pulido, F., Rutigliano, F.A., Quattrini, P., Castaldi, S. (2021). Critical range of soil organic carbon in southern europe lands under desertification risk. J. Environ. Manage. 287, 112285. Doi:10.1016/j.jenvman.2021.112285.
43. Guerra, C.A., Maes, J., Geijzendorffer, I., Metzger, M.J. (2016). An assessment of soil erosion prevention by vegetation in Mediterranean Europe: Current trends of ecosystem service provision. Ecol. Indic. 60, 213-222. Doi: 10.1016/j.ecolind.2015.06.043.
44. Khelifa, W.B., Hermassi, T., Strohmeier, S., Zucca, C., Ziadat, F., Boufaroua, M., Habaieb, H. (2017). Parameterization of the effect of bench terraces on runoff and sediment yield by swat modeling in a small semi-arid watershed in northern Tunisia. Land Degrad. Dev. 28 (5), 1568–1578. Doi:10.1002/ldr.2685.
45. Kosmas, C., Danalatos, N., Cammeraat, L.H., Chabart, M., Diamantopoulos, J., Farand, R., Gutierrez, L., Jacob, A., Marques, H., Martinez-Fernandez, J., Mizara, A., Moustakas, A. (1997). The effect of land use on runoff and soil erosion rates under Mediterranean conditions. Catena 29(1): 45–59. Doi: 10.1016/S0341-8162(96)00062-8
46. Herrera, S., Fernandez, J., Gutierrez, J.M. (2016). Update of the Spain02 Gridded Observational Dataset for Euro-CORDEX evaluation: Assessing the Effect of the Interpolation Methodology. Int. J. Climatol. 36, 900-908. Doi:10.1002/joc.4391.
47. Herrera, S., Gutierrez, J.M., Ancell, R., Pons, M.R., Frias, M.D., Fernandez, J. (2012). Development and analysis of a 50-year high-resolution daily gridded precipitation dataset over Spain (Spain02). Int. J. Climatol. 32, 74-85. Doi:10.1002/joc.2256.
48. Herrera, S., Margarida Cardoso, R., Matos Soares, P., Espirito-Santo, F., Viterbo, P., Gutierrez, J. M. (2019). Iberia01: A new gridded dataset of daily precipitation and temperatures over Iberia. Earth Syst. Sci. Data. 11(4), 1947-1956. Doi:10.5194/essd-11-1947-2019.
49. IPCC: Intergovernmental Panel on Climate Change (2014). Climate Change 2014: synthesis report. Contribution of working groups I, II and II to the Fifth Assessment Report of the Intergovernmental Panel on CC. IPCC, Geneva, Switzerland, 151 pp.
50. IPCC, 2021: Climate Change 2021: The Physical Science Basis. Contribution of Working Group I to the Sixth Assessment Report of the Intergovernmental Panel on Climate Change [Masson-Delmotte, V., P. Zhai, A. Pirani, S.L. Connors, C. Pean, S. Berger, N. Caud, Y. Chen, L. Goldfarb, M.I. Gomis, M., Huang, K,. Leitzell, E., Lonnoy, J.B.R., Matthews, T.K., Maycock, T., Waterfield, O., Yelekci, R., Yu, B., Zhou (eds.)]. Cambridge University Press. In Press.
51. Laflen, J.M., Elliot, W.J., Flanagan, D.C., Meyer, C. R., Nearing, M.A. (1997). WEPP-predicting water erosion using a process-based model. J. Soil Water Conserv. 52(2), 96-102.
52. Lal, R. (2019). Accelerated soil erosion as a source of atmospheric $CO_2$. Soil Till. Res. 188, 35-40. Doi:10.1016/j.still.2018.02.001.
53. Maltsev, K., Yermolaev, O. (2020). Assessment of soil loss by water erosion in small river basins in

Russia. Catena 195, 104726. Doi:10.1016/j.catena.2020.104726.
54. Mancino, G., Nole, A., Salvati, L., Ferrara, A. (2016). In-between forest expansion and cropland decline: A revised USLE model for soil erosion risk under land-use change in a Mediterranean region. Ecol. Ind. 71, 544-550. Doi:10.1016/j.ecolind.2016.07.040.
55. Markhi, A., Laftouhi, N., Grusson, Y., Soulaimani, A. (2019) Assessment of potential soil erosion and sediment yield in the semi-arid N'fis basin (High Atlas, Morocco) using the SWAT model. Acta Geophys. 67, 263–272 (2019). DOI:10.1007/s11600-019-00251-z.
56. Morgan, R.P.C., Quinton, J.N., Smith, R.E., Govers, G., Poesen, J.W.A., Auerswald, K., Chisci, G., Torri, D., Styczen, M.E. (1998). The European soil erosion model (EUROSEM): A dynamic approach for predicting sediment transport from fields and small catchments. Earth Surf. Process. Landf. 23(6), 527-544. Doi:10.1002/(SICI)1096-9837(199806)23:6<527::AID-ESP868>3.0.CO;2-5.
57. Maruffi, L., Stucchi, L., Casale, F., Bocchiola, D. (2022). Soil erosion and sediment transport under climate change for Mera river, in Italian alps of Valchiavenna. Sci. Tot. Environ. 806 DOI:10.1016/j.scitotenv.2021.150651.
58. Moriasi, D., Arnold, J., Van Liew, M., Bingner, R., Harmel, R., Veith, T. (2007). Model evaluation guidelines for systematic quantification of accuracy in watershed simulations. Trans. ASABE 50 (3), 885–900. Doi:10.13031/2013.23153.
59. Moriondo, M., Good, P., Durao, R., Bindi, M., Giannakopoulos, C., Corte-Real, J. (2006). Potential impact of climate change on fire risk in the Mediterranean area. Clim. Res. 31(1), 85-95. Doi: 10.3354/cr031085.
60. Neitsch, S., Arnold, J., Kiniry, J., Williams, J. (2000). Soil and Water Assessment Tool Theoretical Documentation 2000. Grassland, Soil and Water Research Laboratory, Agricultural Research Service, 808 East Blackland Road, Temple, Texas 76502:506.
61. Nunes, A.N., de Almeida, A.C., Coelho, C.O.A. (2011). Impacts of land use and cover type on runoff and soil erosion in a marginal area of Portugal. Appl. Geography 31(2), 687-699. Doi:10.1016/j.apgeog.2010.12.006.
62. Nunes, J.P., Jacinto, R., Keizer, J.J. (2017). Combined impacts of climate and socio-economic scenarios on irrigation water availability for a dry Mediterranean reservoir. Sci. Tot. Environ. 584-585, 219-233. Doi:/10.1016/j.scitotenv.2017.01.131.
63. Nunes, J.P., Seixas, J., Pacheco, N.R. (2008). Vulnerability of water resources, vegetation productivity and soil erosion to CC in Mediterranean watersheds. Hydrol. Proces. 22(16), 3115-3134. Doi:10.1002/hyp.6897.
64. Palm, C., Blanco-Canqui, H., DeClerck, F., Gatere, L., Grace, P. (2014). Conservation agriculture and ecosystem services: An overview. Agric. Ecosyst. Environ. 187, 87-105. Doi:10.1016/j.agee.2013.10.010.
65. Panagos, P., Borrelli, P., Meusburger, K., Alewell, C., Lugato, E., Montanarella, L. (2015a). Estimating the soil erosion cover-management factor at the European scale. Land use Policy 48, 38-50. Doi:10.1016/j.landusepol.2015.05.021.
66. Panagos, P., Borrelli, P., Poesen, J., Ballabio, C., Lugato, E., Meusburger, K., Montanarella, L., Alewell, C., (2015b). The new assessment of soil loss by water erosion in Europe. Environ. Sci. Pol. 54, 438–447. Doi:10.1016/j.envsci.2015.08.012.
67. Panagos, P., Ballabio, C., Himics, M., Scarpa, S., Matthews, F., Bogonos, M., Poesen, J., Borrelli, P. (2021). Projections of soil loss by water erosion in Europe by 2050. Environ. Sci. Policy. 124, 380-392. Doi:10.1016/j.envsci.2021.07.012.
68. Pinto-Correia, T., Mascarenhas, J. (1999). Contribution to the extensification/intensification debate: new trends in the Portuguese montado. Landscape Urban Plan. 46(1), 125-131. Doi: 10.1016/S0169-2046(99)00036-5.
69. Raclot, D., Le Bissonnais, Y., Annabi, M., Sabir, M. (2016). Sub-chapter 2.3.3. Challenges for mitigating Mediterranean soil erosion under global change. In: The Mediterranean region under CC. ISBN: 9782709922203. Doi:10.4000/books.irdeditions.23538.
70. Ramos, C., Reis, E. (2001). As cheias no sul de Portugal em diferentes tipos de bacias hidrograficas.

Finisterra 36(71), 61–82. Doi:10.18055/Finis1648.
71. Renard, K.G., Foster, G.R., Weesies, G.A., McCool, D.K., Yoder, D.C. (1997). Predicting soil erosion by water. A guide to conservation planning with the revised universal soil loss equation (RUSLE), United States Department of Agriculture, Agricultural Research Service (USDA-ARS) Handbook 703. United States Government Printing Office, Washington, DC.
72. Ribeiro, E., Batjes, N.H., van Oostrum, A.J.M. (2020). World Soil Information Service (WoSIS) - Towards the standardization and harmonization of world soil data. Procedures Manual 2020. ISRIC report 2020/01, ISRIC - World Soil Information, Wageningen, 166 p.
73. Roxo, M.J., Casimiro, P.C. (2004). Long term monitoring of soil erosion by water Vale Formoso Erosion Centre—Portugal. In SCAPE- Soil Conservation and Protection for Europe, SCAPE Project Office IBED – Physical Geography: Amsterdam, The Netherlands; 37–48.
74. Savory, A., Butterfield, J. (1999). Holistic Managment: a New Framwork for Decision Making. Island Press, Washington D.C.
75. Schnabel, S., Dahlgren, R.A., Moreno-Marcos, G. (2013). Soil and water dynamics. In Mediterranean Oak Woodland Working Landscapes, Campos P, Huntsinger L, Oviedo Pro JL, Starrs PF, Diaz M, Standiford RB, Montero G (eds). Springer: The Netherland; 91–121.
76. Serpa, D., Nunes, J. P., Santos, J., Sampaio, E., Jacinto, R., Veiga, S., Lima, J.C., Moreira, M., Corte-Real, J., Keizer, J.J., Abrantes, N. (2015). Impacts of climate and land use changes on the hydrological and erosion processes of two contrasting Mediterranean catchments. Sci. Tot. Environ. 538, 64-77. Doi:10.1016/j.scitotenv.2015.08.033.
77. SNIRH: Sistema Nacional de Informacao de Recursos Hidricos (2006). Available online at: https://snirh.apambiente.pt/.
78. Soares, P.M., Cardoso, R.M., Lima, D.C., Miranda, P.M. (2017). Future precipitation in Portugal: high-resolution projections using WRF model and EURO-CORDEX multi-model ensembles. Clim. Dynam. 49(7-8), 2503-2530. Doi: 10.1007/s00382-016-3455-2.
79. Soussana, J.F., Tallec, T., Blanfort, V. (2010). Mitigation the greenhouse gas balance of ruminant production systems through carbon sequestration in grasslands. Animal 4, 334–350. Doi: 10.1017/S1751731109990784
80. Steinhoff-Knopp, B., Kuhn T.K., Burkhard, B. (2021). The impact of soil erosion on soil-related ecosystem services: development and testing a scenario-based assessment approach. Environ. Monit. Assess. 274. Doi.org/10.1007/s10661-020-08814-0.
81. Tasdighi, A., Arabi, M., Harmel, D. (2018). A probabilistic appraisal of rainfall-runoff modeling approaches within SWAT in mixed land use watersheds. J. Hydrol. 564, 476–489. Doi:10.1016/j.jhydrol.2018.07.035.
82. USDA: United States Department of Agriculture (2004). National Engineering Handbook, Part 630 – Hydrology, Chapter 9: Hydrologic Soil-Cover Complexes.
83. Vanwalleghem, T., Amate, J. I., de Molina, M. G., Fernandez, D. S., Gomez. J. A. (2011) .Quantifying the effect of historical soil management on soil erosion rates in Mediterranean olive orchards Agric. Ecosyst. Environ. 142 (3–4), 341-351. Doi:10.1016/j.agee.2011.06.003.
84. Verheijen, F.G.A., Jones, R.J.A., Rickson, R.J., Smith, C.J. (2009). Tolerable versus actual soil erosion rates in Europe. Earth-Science Rev. Doi:10.1016/j.earscirev.2009.02.003.
85. Whitehead, D. (2020). Management of Grazed Landscapes to Increase Soil Carbon Stocks in Temperate, Dryland Grasslands. Front. Sustain. Food Syst. 4. Doi:10.3389/fsufs.2020.585913.
86. Williams, J.R. (1995). Chapter 25: The EPIC Model. In: Singh, V.P. (Ed.), Computer Models of Watershed Hydrology. Water Resources Publications, Highlands Ranch, U.S., pp. 909–1000.
87. Wischmeier, W.H., Smith, D.D. (1978). Predicting rainfall erosion losses – a guide for conservation planning. U.S. Department of Agriculture, Agriculture Handbook 537.
88. Yang, D., Kanae, S., Oki, T., Koike, T., Musiake, K. (2003). Global potential soil erosion with reference to land use and CCs. Hydrol. Proces. 17(14), 2913-2928. Doi:10.1002/hyp.1441.
89. Yassoglou, N.J., Kosmas, C. (2000). Desertification in the Mediterranean Europe: a case in Greece. Rala Report No. 200.

90. Zhao, G., Mu, X., Wen, Z., Wang, F., Gao, P. (2013). Soil erosion, conservation, and eco-environment changes in the loess plateau of china. Land Degrad. Dev. 24(5), 499-510. Doi:10.1002/ldr.2246.
91. Zittis, G., Hadjinicolaou, P., Klangidou, M., Proestos, Y., Lelieveld, J. (2019). A multi-model, multi-scenario, and multi-domain analysis of regional climate projections for the Mediterranean. Reg. Environ. Change 19, 2621–2635. Doi:10.1007/s10113-019-01565-w.